Journal of Quantitative Spectroscopy & Radiative Transfer 207 (2018) 1–7

Contents lists available at ScienceDirect

Journal of Quantitative Spectroscopy & Radiative Transfer

journal homepage: www.elsevier.com/locate/jqsrt

# Line intensities of the 30011e – 00001e band of $^{12}C^{16}O_2$ by laser-locked cavity ring-down spectroscopy

P. Kang[a], J. Wang[a], G.-L. Liu[a], Y.R. Sun[a,b], Z.-Y. Zhou[c], A.-W. Liu[a,b,*], S.-M. Hu[a,b]

[a] Hefei National Laboratory for Physical Sciences at Microscale, iChem Center, University of Science and Technology of China, Hefei 230026, China
[b] CAS Center for Excellence and Synergetic Innovation Center in Quantum Information and Quantum Physics, University of Science and Technology of China, Hefei 230026, China
[c] National Institute of Metrology, Beijing 100013, China

ARTICLE INFO

*Article history:*
Received 31 October 2017
Revised 18 December 2017
Accepted 18 December 2017
Available online 19 December 2017

*Keywords:*
Carbon dioxide
Cavity ring-down spectroscopy
Line intensities

ABSTRACT

Thirty well isolated ro-vibrational transitions of the 30011e – 00001e band of $^{12}C^{16}O_2$ at 1.54 $\mu$m have been recorded with a laser-locked cavity ring-down spectrometer. The line intensities were obtained with accuracies better than 0.85%. Comparisons of the line intensities determined in this work with literature experimental values and those from HITRAN2016, AMES, UCL-IAO and CDSD-296 line lists are given.



## 1. Introduction

As the second most abundant greenhouse gas in Earth's atmosphere, carbon dioxide currently has a global average concentration of 404 parts per million by volume [1]. The terrestrial atmospheric concentration of carbon dioxide has increased almost 43 percent since pre-industrial times due to human activities. Its significant role in climate change impels several agencies to launch space-based observations of carbon dioxide, for example OCO-2 (USA) [2], GOSAT (Japan) [3], ASCENDS (USA) [4], Tan–Sat (China) [5], to monitor $CO_2$ global levels and their variations. These projects aim to retrieve the atmospheric column-averaged $CO_2$ dry air mole fraction ($XCO_2$) with precisions in the range of 0.25∼1%. These remote sensing activities heavily depend on the molecular absorption model used within the retrievals, therefore the accuracy of the line parameters and line profiles. To fulfill the goals of the current missions, the accuracy of $CO_2$ line intensities are required to reach 0.3∼0.5% [6].

Line intensities are much more difficult to be determined accurately than line positions. Along with the development of high-precision laser spectroscopy techniques and the significant progress of line profile models, the accuracy of $CO_2$ line intensities determined at the laboratory has fulfilled the requirements for modern atmospheric remote sensing experiments [7–13]. However, only several studies [10] accessed to obtain a few lines with a precision of 0.3-1%. In the meantime, attempts [12,14–20] have been made to provide high-accuracy theoretical line intensities for $CO_2$. For instance, Huang et al. [14–17] has performed a series of *ab initio* studies, obtained the most accurate potential energy surface (PES) of $CO_2$, and generated the infrared line lists for 13 $CO_2$ isotopologues denoted as AMES [16,17]. Tennyson's group from University College London have shown that it is possible to derive computed line intensities using *ab initio* calculated dipole moment surface (DMS) with an accuracy comparable to available measurements for tri-atomic molecules such as the water molecule, hydrogen ion and carbon dioxide [12,21–24]. The agreement at the 0.3% level between *ab initio* computations and high-accuracy experiments [12] for $^{12}C^{16}O_2$ indicates the possibility of the atmospheric remote sensing research using *ab initio* calculations. Another set of calculated $CO_2$ line lists, named as UCL-IAO list, for 13 isotopologues of carbon dioxide has been produced by Zak et al. [19,25,26] with the combination of the high accuracy *ab initio* DMS [12] and the methodology used in Ref. [21]. Meanwhile, an empirical carbon dioxide spectroscopic databank (CDSD-296) [18,19] in the spectral range of 6–14,075 $cm^{-1}$ has been created by Tashkun et al. within the framework of effective operators and based on the global weighted fit of spectroscopic parameters to the observed data from more than 200 measured spectra with uncertainties varying between ∼0.1% [8] and over 100% [27]. It leads to a high percentage of line intensities in CDSD databank with the stated un-

* Corresponding author at: Hefei National Laboratory for Physical Sciences at Microscale, iChem Center, University of Science and Technology of China, Hefei 230026, China.
*E-mail address:* awliu@ustc.edu.cn (A.-W. Liu).

https://doi.org/10.1016/j.jqsrt.2017.12.013
0022-4073/

certainty of 20% or worse, which are still too high for remote sensing activities.

Recently, the widely-used molecular spectroscopic database HITRAN has been updated to the 2016 version [28]. The intensities of most lines in the 0-8000 $cm^{-1}$ region in the latest database have been provided by UCL-IAO since similar accuracy can be given for all isotopologues by using the variational approach in the UCL-IAO line-list. Recent high-precision near-IR spectroscopic measurements in the 1.6 $\mu$m [10,12] and 2.0 $\mu$m [13,29] have experimentally confirmed that the UCL-IAO line list is accurate to the sub-percent level. Some lines in the UCL-IAO list, the so-called "sensitive" bands involving vibrational states with strong resonances, have been replaced with the data from CDSD-296 [19], such as the 30011e – 00001e, 13311e – 13302e, 40012e – 00001e, 40011e – 00001e bands of the key $CO_2$ isotopologue [20]. For the transitions with line intensity larger than $1 \times 10^{-27}$ $cm^{-1}$/ (molecule $cm^{-2}$) in the 30011e – 00001e band of $^{12}C^{16}O_2$, there is an average difference of 3.5% - 7.8% between UCL-IAO and CDSD-296. The CDSD-296 values agree well with Toth's experimental values [30] within stated uncertainties of 2.4% for most observed lines, but are 5% weaker than the observed values retrieved by cavity ring-down spectroscopy (CRDS) in Grenoble [18] for the transitions of $J' > 48$. However, the UCL-IAO data agree better with the observed values in Ref. [18] for the transitions with intensity weaker than $2 \times 10^{-26}$ $cm^{-1}$/(molecule $cm^{-2}$). For this reason, an independent high-accuracy line intensity measurement is needed for the transitions of the 30011e – 00001e band of $^{12}C^{16}O_2$.

In the present work, the line intensities of thirty transitions with no interference from other absorption lines have been recorded by a laser-locked cavity ring-down spectrometer with high precision as well as high sensitivity. This spectrometer is similar to the experimental set-ups developed in Refs. [31,32]. High-precision line intensities are retrieved from the recorded spectra with a relative uncertainty of 0.7% on average, which was considerably improved over our previous studies on $CO_2$ and $N_2O$ around 780 nm [33,34]. Precise intensities of the lines in the 30011e – 00001e "sensitive" band will be useful for the evaluation of the HITRAN2016, CDSD-296, AMES and UCL-IAO database.

## 2. Experimental details

The diagram of the experimental setup is presented in Fig. 1, which consists of frequency locking and spectral probing. A tunable external-cavity diode laser (ECDL, Toptica DL Pro-1550) is split into two beams by a polarizing beam splitting cube. The s-polarization beam is locked to a temperature-stabilized ring-down (RD) cavity using the Pound–Drever-Hall (PDH) method. The RD cavity is composed of two high-reflectivity mirrors with a distance of 110.8 cm. Each mirror has a reflectivity of 99.996% at 1.5-1.7 µm (Layertec GmbH). Therefore, the RD cavity has a finesse of about $7.8 \times 10^4$ and a mode width of about 1.6 kHz. The RD cavity is made of Invar, located in a stainless-steel vacuum chamber. A feedback circuit controls the heating-current in a wire surrounding the stainless-steel chamber to stabilize the Invar cavity temperature at about 298.8 K which was measured with two calibrated platinum thermal sensors attached at two sides of the RD cavity. We used a frequency counter (Agilent 53181A) to monitor the beat frequency between the laser and a frequency comb, and the results are shown in Fig. 2(a). The comb is synthesized by an Er: fiber oscillator operated at 1.56 $\mu$m. The repetition frequency and carrier offset frequency of the comb are locked to precise radio-frequency sources referenced to a GPS-disciplined rubidium clock (SRS FS725). The beat signal has a long-term drift of about 1 MHz per h, which is consistent with the thermal expansion of the cavity under a temperature drift of 50 mK. The temperature uncertainty of the RD cavity was estimated to be 0.2 K at maximum taking into account the temperature non-uniformity along the RD cavity. The frequency calibration of the observed spectrum was based on the precise measurement of the RD cavity's free spectral range (FSR). Fig. 2(b) shows FSR of the empty cavity obtained from the positions of two cavity modes. The FSR value was determined to be 135272623.7(5) Hz, with a maximum fluctuation of about 2 Hz within three hours. It is worth to mention that the dispersion due to sample absorption [35] have been considered in our measurements.

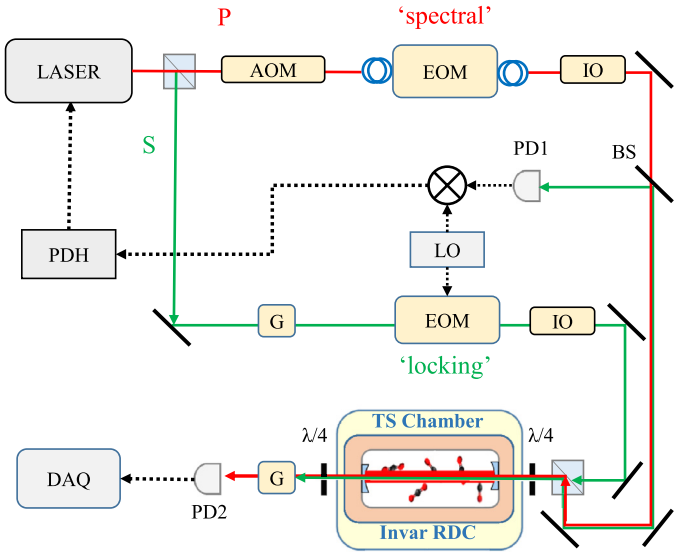


**Fig. 1.** Configuration of the experimental setup. AOM: acoustic-optical modulator; BS:50:50 beam splitter; DAQ: data acquisition system; EOM: electro-optical modulator; G:Glan-Taylor prism; LO: local oscillator; PBS: polarizing beam splitter; PD: photodiode detector; QWP: quarter- wave plate; SG: signal generator; TS: temperature stabilized.

**Table 1**
Pressure series list for line intensity measurements of 30011e - 00001e band of $^{12}C^{16}O_2$.

| Series | 1 (Pa) | 2 (Pa) | 3 (Pa) | 4 (Pa) | Relative uncertainty |
|---|---|---|---|---|---|
| a | 5.00 | 6.22 | 8.47 | 9.97 | 0.7% |
| b | 22.88 | 31.51 | 37.49 | 59.01 | 0.3% |
| c | 100.18 | 120.64 | 676.20 | 800.60 | 0.25% |

The p-polarization beam passes an acousto-optic modulator (AOM) and a fiber electro-optic modulator (EOM). The EOM modulation frequency is stepped in increments of the RD cavity's free spectral range to record the spectrum. A single selected sideband of EOM is then coupled into the high-finesse cavity to produce the ring-down signal detected by an avalanche photodiode detector (APD) with a combination of polarizing waveplates and Glan–Tylor prisms. When the signal reaches a steady level, it triggers an AOM to block the probe laser beam to initiate a ring-down event. The ring-down curve is fit by an exponential decay function to derive the decay time $\tau$, and the sample absorption coefficient $\alpha$ is determined according to the equation $\alpha = (c\tau)^{-1}$-$(c\tau_0)^{-1}$, where $c$ is the speed of light and $\tau_0$ is the decay time of an empty cavity. Fig. 3(a) shows the recorded $(c\tau)^{-1}$ value of the empty cavity, and the corresponding Allan deviation is given in Fig. 3(b). The limit of detection, presented as the minimum detectable absorption coefficient, reaches about $4.8 \times 10^{-12}$ $cm^{-1}$at an averaging time of about 30 s.

Natural carbon dioxide sample gas with a stated purity of 99.995% was bought from the Nanjing Special Gas Co. and further purified by a "freeze-pump-thaw" process before use. Three pressure series, listed in Table 1, were adopted to reduce the statisti-

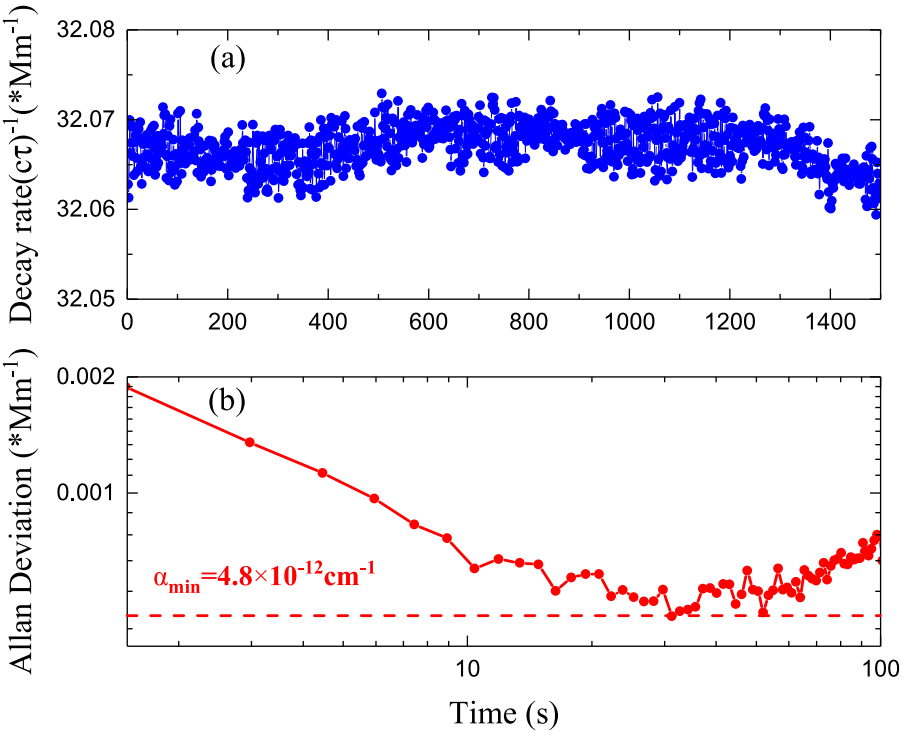


**Fig. 2.** The Free spectral range (FSR) precision. (a) Beat frequency between the probe laser and the frequency comb. Data are shifted for better illustration. (b) FSR values of the empty cavity determined by measuring the position difference of two cavity modes.

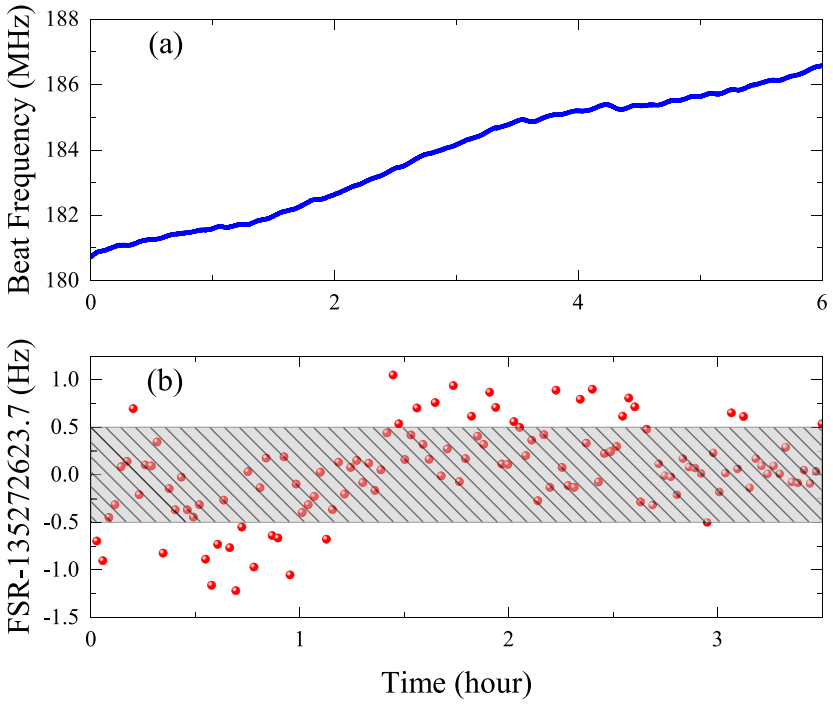


**Fig. 3.** The sensitivity of the CRDS instrument. (a) Absorption coefficient detected with an empty cavity. (b) Allan deviation of the data shown in (a).

cal uncertainty. Sample pressures were measured by capacitance gauges Pfeiffer Vacuum CCR364 (full range 1 Torr) and CCR 372 (full range 100 Torr) with stated accuracies of 0.2% and 0.15%, respectively. The pressure gauges were calibrated at National Institute of Metrology, China. The absolute relative uncertainties at different pressure series are also given in Table 1. To avoid the interference from neighbor absorptions of other molecules and isotopologues, only thirty well-isolated transitions in the 30011e – 00001e band were studied in this work. The absorption spectra of 30 lines were recorded at four different pressures of a respective series, and 30 times at each pressure.

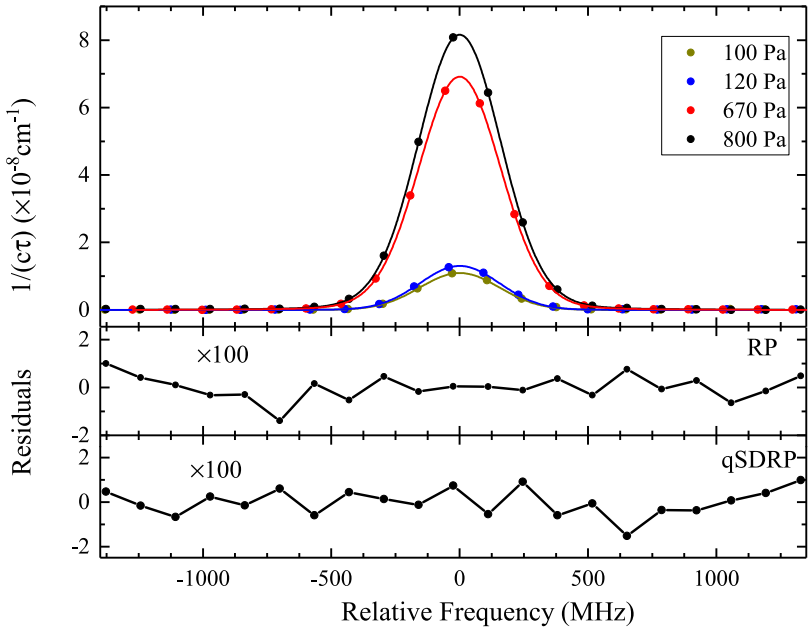


**Fig. 4.** Example of CRDS-spectrum for the R (62) lines, along with the residuals retrieved with Rautian and qSDRP profiles.

## 3. Results

### 3.1. Line intensity retrieval

The spectra were recorded at sample pressures of 0.005 to 0.8 kPa, the ratio $\Gamma_L/\Gamma_D$ of the Lorentzian (calculated values with Hitran2016) to Doppler widths varies from 0.011 to 0.09 in a narrow pressure range. It is hard to remove the partial correlations between various parameters used in the partially-Correlated quadratic-Speed-Dependent Hard-Collision (pCqSDHC) profile [36]. Casa et al. [37] and Long et al. [38] have concluded that the line parameters including the integrated absorbance and Lorentzian widths obtained from fitting using the "hard" -collision Rautian (RP) [39] profile are very close to those obtained from fitting the same spectrum using the speed-dependent Nelkin–Ghatak profile (SDNGP) [40]. In this case, the spectrum recorded with pressure series a and b were fitted with the Voigt profile, while the Rautian profile was adopted for the spectrum of transitions weaker than $4\times10^{-26}$ cm$^{-1}$/(molecule cm$^{-2}$). The Doppler width was fixed at the calculated value. The line center, intensity, collision broadening width, Dicke narrowing coefficient and the parameters for baseline were derived from the fit. Fig. 4(a) shows the spectra of the R (62) line recorded with sample pressures in the range between 100.18 and 800.60 Pa. The fitting residuals of the measured spectra at 800.60 Pa is also presented in Fig. 4(b).

The line intensity $S(T_0)$ in cm$^{-1}$/(molecule cm$^{-2}$) at the standard temperature $T_0=296$ K can be given by the following equation:

$$S(T_0)=\frac{1}{4\pi\varepsilon_0}\frac{8\pi^3\nu_0}{3hcQ(T_0)}|R|^2L(J)e^{-hcE''/k_BT_0}[1-e^{-hc\nu_0/k_BT_0}] \quad (1)$$

In Eq. (1), $1/4\pi\varepsilon_0=10^{-36}$ erg cm$^3$ D$^{-2}$; $h$ is the Planck constant; $c$ is the speed of light; $\nu_0$ is the transition wavenumber in cm$^{-1}$; $E''$ is the lower level energy in cm$^{-1}$; and $k_B$ is the Boltzmann constant. The Hönl–London factor $L(J)$ is equal to $|m|$, where $m$ is $-J$ for P branch transitions, and $J+1$ for R branch. The rotational dependence of the transition dipole moment squared $|R|^2$ can be expressed as:

$$|R|^2=|R_0|^2(1+A_1m+A_2m^2)^2 \quad (2)$$

Where $|R_0|^2$ is the vibrational transition dipole moment squared, $A_1$ and $A_2$ are the Herman-Wallis coefficients. The calculated values of the total partition function, $Q(T_0)$, is 286.094 at $T_0=296$ K, and $Q$(T) is 289.5 at T = 298.8 K for $^{12}C^{16}O_2$ from TIPS_2017 [41].

The line intensities of thirty lines in the 30011e – 00001e band of $^{12}C^{16}O_2$ are given in Table 2 with natural abundance of 0.9842 and temperature at 296 K. The statistical uncertainty obtained from the fit, the rotational dipole moment squared $|R|^2$ and pressure series for each transition are also included in Table 2. The vibrational transition dipole moment $|R_0|^2$ and the Herman-Wallis coefficients are determined to be $2.0761(41)\times10^{-8}$ Debye$^2$, $3.30(25)\times10^{-4}$ and $-3.809(76)\times10^{-5}$ from the fit according to Eq. (2). The relative difference between the experimental line intensities and calculated values with the Herman–Wallis coefficients are also given in Table 2.

### 3.2. Estimated overall error budget

The uncertainty of the line intensity is composed of statistic and systematic uncertainties. The former one was determined from the least-squares fits. The systematic uncertainty sources include (i) isotopologue abundance, (ii) pressure, (iii) temperature, (iv) baseline polynomial fit, and (v) line profile model.

(i) In order to estimate the systematic uncertainty arising from the abundance of $^{12}C^{16}O_2$, we determined other minor isotopologue abundance of carbon dioxide in the sample. The absorption spectrum of transitions located at 6264.707 cm$^{-1}$ and 6447.248 cm$^{-1}$ were recorded to obtain the isotopologue abundance of $^{13}C^{16}O_2$ and $^{12}C^{16}O^{18}O$, respectively. They were determined to be 1.09% and 0.39% using the experimental line intensities given by Toth et al. [42] and Karlovets et al. [43]. The ratio between these two abundances agrees well with the natural abundance ratio of 0.01106: 0.00395. On the other side, the isotopologue abundance of carbon dioxide in the sample were measured with a residual gas analyzer (Stanford Research System: RGA 100) based on mass spectrometry (MS) method. The measured abundances of carbon dioxide isotopolgues with masses of 44 ($^{12}C^{16}O_2$), 45 ($^{13}C^{16}O_2$ and $^{12}C^{16}O^{17}O$), 46 ($^{12}C^{12}O^{18}O$, $^{13}C^{16}O^{17}O$ and $^{12}C^{17}O_2$) are in the ratio of 0. 9843: 0.0116: 0.0040, which also agree well with the

**Table 2**
Measured line Intensities of 30011e - 00001e band of $^{12}C^{16}O_2$.

| Line | *Exp.* intensity | *Exp.* uncertainty % *Statis.* | *Sys.* | Unweighted $\|R\|^2 \times 10^{-8}$ | *(o-c)*% | Pressure series |
|---|---|---|---|---|---|---|
| P 64 | 3.227(21)E-27 | 0.3 | 0.6 | 1.713(11) | 0.2 | c |
| P 62 | 5.190(31)E-27 | 0.3 | 0.6 | 1.740(10) | 0.6 | c |
| P 56 | 1.933(11)E-26 | 0.3 | 0.5 | 1.803(10) | 0.7 | c |
| P 52 | 4.236(20)E-26 | 0.1 | 0.5 | 1.830(09) | 0.2 | b |
| P 48 | 8.710(39)E-26 | 0.1 | 0.4 | 1.864(09) | 0.2 | b |
| P 42 | 2.236(09)E-25 | 0.1 | 0.4 | 1.900(08) | −0.4 | b |
| P 40 | 2.957(12)E-25 | 0.1 | 0.4 | 1.912(08) | −0.5 | b |
| P 38 | 3.841(15)E-25 | 0.1 | 0.4 | 1.925(08) | −0.6 | b |
| P 32 | 7.587(62)E-25 | 0.4 | 0.7 | 1.978(16) | 0.2 | a |
| P 30 | 9.137(76)E-25 | 0.4 | 0.7 | 1.990(16) | 0.3 | a |
| P 26 | 1.244(10)E-24 | 0.4 | 0.7 | 2.009(16) | 0.2 | a |
| P 24 | 1.403(11)E-24 | 0.4 | 0.7 | 2.014(16) | 0.0 | a |
| P 20 | 1.671(13)E-24 | 0.4 | 0.7 | 2.030(16) | 0.0 | a |
| P 14 | 1.774(14)E-24 | 0.4 | 0.7 | 2.048(16) | −0.2 | a |
| P 8 | 1.333(11)E-24 | 0.4 | 0.7 | 2.059(17) | −0.3 | a |
| P 4 | 7.397(60)E-25 | 0.4 | 0.7 | 2.065(17) | −0.3 | a |
| R 4 | 9.289(74)E-25 | 0.4 | 0.7 | 2.073(17) | −0.2 | a |
| R 6 | 1.247(10)E-24 | 0.4 | 0.7 | 2.074(17) | −0.2 | a |
| R 12 | 1.857(15)E-24 | 0.4 | 0.7 | 2.072(17) | 0.0 | a |
| R 14 | 1.930(16)E-24 | 0.4 | 0.7 | 2.072(17) | 0.2 | a |
| R 16 | 1.937(16)E-24 | 0.4 | 0.7 | 2.069(17) | 0.2 | a |
| R 18 | 1.889(15)E-24 | 0.4 | 0.7 | 2.067(16) | 0.3 | a |
| R 20 | 1.794(14)E-24 | 0.4 | 0.7 | 2.065(16) | 0.5 | a |
| R 28 | 1.149(09)E-24 | 0.4 | 0.7 | 2.045(16) | 0.8 | a |
| R 34 | 6.603(52)E-25 | 0.3 | 0.7 | 2.024(16) | 1.0 | a |
| R 36 | 5.297(43)E-25 | 0.4 | 0.7 | 2.021(16) | 1.4 | a |
| R 52 | 4.533(22)E-26 | 0.1 | 0.5 | 1.897(10) | 0.4 | b |
| R 56 | 2.058(11)E-26 | 0.2 | 0.5 | 1.860(10) | 0.1 | c |
| R 62 | 5.523(33)E-27 | 0.2 | 0.6 | 1.795(11) | −0.6 | c |
| R 64 | 3.433(22)E-27 | 0.3 | 0.6 | 1.766(12) | −1.1 | c |

*Exp.* intensity is experimental line intensity in $cm^{-1}$/(molecule $cm^{-2}$) at 296 K for natural abundance of $^{12}C^{16}O_2$ (0.9842).
*Statis.* is the statistical relative uncertainty; *Sys.* is the systematical contribution from abundance, pressure, temperature, baseline and line profile model.
*(o − c)%* is the relative difference between the experimental line intensity and calculated value with the Herman–Wallis coefficients.

natural abundance ratio of 0.98420: 0.01179: 0.00395. Considering the line intensity uncertainties of these two transitions, the relative uncertainty introduced by the isotopologue abundance is assumed to be 3% for these two isotopologues. It causes less than 0.03% uncertainty for the abundance of $^{12}C^{16}O_2$. The determined $^{12}C^{16}O_2$ abundance agrees with the natural abundance within $1\sigma$ variation. Therefore, the natural value is adopted here, and the uncertainty of 0.03% contributes to the systematic errors.

(ii) The pressure uncertainties of 0.25% ∼ 0.7% listed in Tables 1 and 2 are taken into account in the systematic errors.

(iii) The temperature relative uncertainty is at the level of 0.07%. It will introduce a systematic error of 0.07% ∼ 0.61% for lines with lower level energies in the range of 7.804 ∼ 1621.003 $cm^{-1}$ based upon the equation:

$$\frac{\Delta S}{S} \cong (1 + \frac{hcE''}{k_B T}) \frac{\Delta T}{T}. \quad (3)$$

Eq. (3) can be derived from the following equation:

$$S(T_0) = \frac{k(T) \times T}{n_0 \times 273.15} \cdot \frac{Q(T)}{Q(T_0)} \cdot \frac{[1 - e^{-hc\nu_0/k_B T_0}]}{[1 - e^{-hc\nu_0/k_B T}]} \cdot e^{-\frac{hcE''}{k_B}(\frac{1}{T_0} - \frac{1}{T})} \quad (4)$$

In Eq. (4), $k(T)$ is the line strength at the unit of cm−1/(cm atm), $n0$ is the *Loschmidt* constant, and $T$ is the experimental temperature.

(iv) The difference between the integrated line absorbance obtained with linear and second-order polynomial baselines is about 0.05%.

(v) The systematic uncertainty caused by using different line profile models can be neglected for 24 lines with line intensities stronger than $4 \times 10^{-26}$ $cm^{-1}$/(molecule $cm^{-2}$), since the spectra were recorded with pressures less than 60 Pa.

We notice that the Dicke narrowing coefficient derived from the fit using RP is one-third of the calculated value related to the mass diffusion coefficient $D$ by $\beta = k_B T/(2\pi cmD)$ with $m$ the molecular mass, within the Lennard–Jones interaction potential [44]. The quality of fit (QF) parameter based on the RP model reduces to 320 with calculated Dicke narrowing value from 1500 with adjustable Dicke-narrowing coefficient. This implies that the Dicke narrowing coefficient calculated by the diffusion theory is not suitable to describe the speed dependent frequency. The spectra recorded at a pressure of 800.6 Pa have also been simulated with speed-dependent Voigt profile (SDVP) and quadratic speed-dependent Rautian profile (qSDRP). Fig. 3(c) shows the fitting residuals with qSDRP. Less than 0.1% difference is found for the integrated absorbance from different line profile models.

The total systematic uncertainties for each line have been calculated, and given in Table 2 together with the statistical uncertainties. The main source of systematic uncertainties is from the pressure for strong line, and from the density population due to the temperature uncertainty for the transitions with high $J'$. The relative uncertainty is less than 0.85% for all the lines.

## 4. Discussion and conclusion

The rotational lines of 30011e – 00001e band have been experimentally studied with Fourier-transform spectroscopy [30,45] and cavity ring-down spectroscopy [18] for the lines stronger than

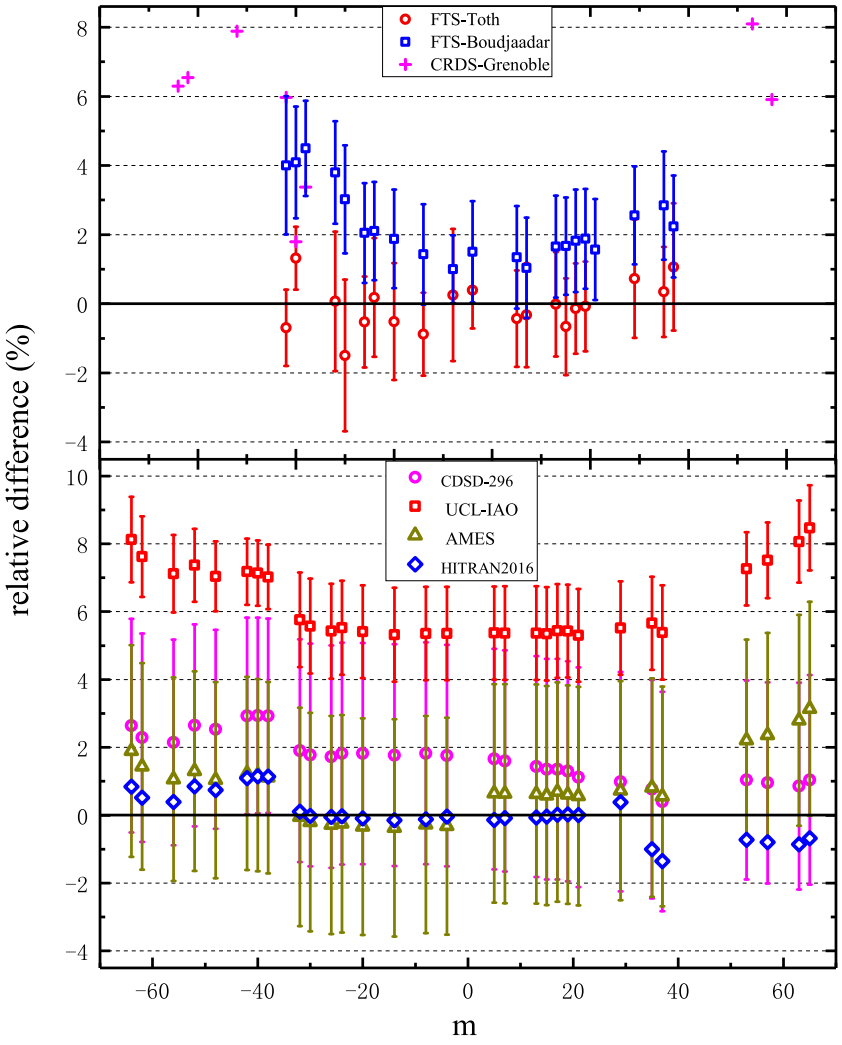


**Fig. 5.** Literature values relative to the present measurements versus the rotational quantum number m for the 30011e – 00001e band of $^{12}C^{16}O_2$. Error bars represent $1\sigma$ standard deviation. Data sources are FTS-Toth [28], FTS-Boudjaadar [43], CRDS-Grenoble [29], HITRAN2016, CDSD-296, ULC-IAO, AMES.

$1 \times 10^{-28}$ cm$^{-1}$/(molecule cm$^{-2}$). The accuracy of the line intensity measured by FTS was assumed to be within 1% for most lines, while down to 4-7% in the CRDS-Grenoble measurement. However, there is a −2.2% deviation on average between the FTS-Toth [30] and FTS-Boujdaadar [45] measurements.

Fig. 5 compares FTS and CRDS-Grenoble experimental values with our measurements in the upper panel. The results are summarized as the relative intensity difference versus rotational quantum number *m*. Our measurements agree well with FTS-Toth values for the lines stronger than $2 \times 10^{-25}$ cm$^{-1}$/(molecule cm$^{-2}$). The deviations of FTS-Boujdaadar values from this work vary from 1% to 4% with the increment of quantum number *J'*. The relative difference between two CRDS measurements is about 6% being within the claimed uncertainty of CRDS-Grenoble.

Comparisons of our experimental line intensities to values archived in HITRAN2016 and CFDSD-296 database, AMES and UCL-IAO *ab initio* calculations are presented in the lower panel of Fig. 5. The average relative difference between HITRAN2016 and the present measured values equals to 0.03% and has a standard deviation of 0.63%. The line intensities in CDSD-296 agree with our measurements within $1\sigma$ combined relative uncertainty, with a deviation of 1.7% on average. The calculated values from AMES line list also agree well with our values for most lines, while the deviations between AMES and our measurements increase to 3% for the transitions with high *J'* values in the R branch. A much larger discrepancy is found for the UCL-IAO line list. For the transitions with quantum number $|m| \leq 36$, UCL-IAO values are 5.5% larger than our measurements on average. The relative difference goes up to 8.5% for the R (64) line. Our measurements show that the calculated line intensities of the 30011e – 00001e band from the UCL-IAO line list are "sensitive", which was also mentioned to be used with caution [19]. High precision measurement of line intensities of other "sensitive" bands will be performed in the future.

## Acknowledgments

This work is jointly supported by the NSFC (Nos. 21473172, 21427804 and 21688102), NBRPC(No. 2013CB834602), and CAS (No. XDB21020100).

## Supplementary materials

Supplementary material associated with this article can be found, in the online version, at doi:10.1016/j.jqsrt.2017.12.013.

## References

[1] National oceanic & atmospheric administration (NOAA)-Earth System Research Laboratory (ESRL), Trends in carbon dioxide: globally averaged marine surface monthly mean data. ftp://aftp.cmdl.noaa.gov/products/trends/co2/co2_mm_gl.txt.

[2] Crisp D, Atlas R, Breon F, Brown L, Burrows J, Ciais P, et al. The orbiting carbon observatory (OCO) mission. Adv Space Res 2004;34:700–9.
[3] Butz A, Guerlet S, Hasekamp O, Schepers D, Galli A, Aben I, et al. Toward accurate $CO_2$ and $CH_4$ observations from GOSAT. Geophys Res Lett 2011;38:L14812.
[4] Abshire JB, Riris H, Allan GR, Weaver CJ, Mao J, Sun X, et al. Approach to measure CO2 concentrations from space for the ASCENDS mission. SPIE 2010; 7832: 78320D.
[5] Liu Y, Duan M, Cai Z, Yang D, Lu D, Yin Z, et al. Chinese carbon dioxide satellite (TanSat) status and plans. In: Proc. of American Geophysical Union 2012 Fall Meeting. American Geophysical Union; 2012.
[6] Miller CE, Crisp D, DeCola PL, Olsen SC, Randerson JT, Michalak AM, Alkhaled A, Rayner P, Jacob DJ, Suntharalingam P, et al. Precision requirements for space-based data. J Geophys Res 2007;112:D10314.
[7] Casa G, Parrett DA, Castrillo A, Wehr R, Gianfrani I. Highly accurate determinations of $CO_2$ line strengths using intensity-stabilized diode laser absorption spectrometry. J Chem Phys 2007;127:084311.
[8] Casa G, Wehr R, Castrillo A, Fasci E, Gianfrani I. The line shape problem in the near-infrared spectrum of self-colliding $CO_2$ molecules: experimental investigation and test of semiclassical models. J Chem Phys 2009;130:184306.
[9] Wuebbeler G, Viquez GJP, Jousten K, Werhahn O, Elster C. Comparison and assessment of procedures for calculating the R(12) line strength of the $\nu_1+2\nu_2+\nu_3$ band of $CO_2$. J Chem Phys 2011;135:204304.
[10] Devi VM, Benner DC, Sung K, Brown LR, Crawford TJ, Miller CE, et al. Line parameters including temperature dependences of self- and air-broadened line shapes of $^{12}C^{16}O_2$: 1.6-$\mu$m region. J Quant Spectrosc Radiat Transfer 2016;177:117–44.
[11] Brunzendorf J, Werwein V, Serduykov A, Werhahn O, Ebert V. $CO_2$ line strengthmeasurements in the 20012-00001 band near 2 µm. In: The 24th colloquium on high resolution molecular spectroscopy; 2015. p. O17.
[12] Polyansky OL, Bielska K, Ghysels M, Lodi L, Zobov NF, Hodges JT, et al. High accuracy $CO_2$ line intensities determined from theory and experiment. Phys Rev Lett 2015;114:243001.
[13] Odintsova TA, Fasci E, Moretti L, Zak EJ, Polyansky OL, Tennyson J, et al. Highly accurate intensity factors of pure CO2 lines near 2 $\mu$m. J Chem Phys 2017;146:244309.
[14] Huang XC, Schwenke DW, Tashkun SA, Lee TJ. An isotopic-independent highly accurate potential energy surface for $CO_2$ isotopologues and an initial $^{12}C^{16}O_2$ infrared line list. J Chem Phys 2012;136:124311.
[15] Huang XC, Freedman RS, Tashkun SA, Schwenke DW, Lee DJ. Semi-empirical $^{12}C^{16}O_2$ IR line lists for simulations up to 1500 K and 20,000 cm$^{-1}$. J Quant Spectrosc Radiat Transfer 2013;130:134–46.
[16] Huang XC, Gamache RR, Freedman RS, Schwenke DW, Lee RJ. Reliable infrared line lists for 13 $CO_2$ isotopologues up to E=18,000 cm$^{-1}$ and 1500 K, with line shape parameters. J Quant Spectrosc Radiat Transfer 2014;147:134–44.
[17] Huang XC, Schwenke DW, Freedman RS, Lee TJ. AMES-2016 line lists for 13 isotopologues of CO2: updates, consistency, and remaining issues. J Quant Spectrosc Radiat Transfer 2017;203:224–41.
[18] Perevalov BV, Campargue A, Gao B, Kassi S, Tashkun SA, Perevalov VI. New CW-CRDS measurements and global modeling of $^{12}C^{16}O_2$ absolute line intensities in the 1.6 $\mu$m region. J Mol Spectrosc 2008;252:190–7.
[19] Tashkun SA, Perevalov VI, Gamache RR, Lamouroux J. CDSD-296, high resolution carbon dioxide spectroscopic databank: version for atmospheric applications. J Quant Spectrosc Radiat Transfer 2015;152:45–73.
[20] Zak E, Tennyson J, Polyansky OL, Lodi L, Zobov NF, Tashkun SA, Perevalov VI. A room temperature $CO_2$ line list with ab initio computed intensities. J Quant Spectrosc Radiat Transfer 2016;177:31–42.
[21] Lodi L, Tennyson J, Polyansky OL. A global high accuracy ab initio dipole moment surface for the electronic ground state of the water molecule. J Chem Phys 2011;135:034113.
[22] Lodi L, Tennyson J. Line lists for $H_2{}^{18}O$ and $H_2{}^{17}O$ based on empirically-adjusted line positions and ab initio intensities. J Quant Spectrosc Radiat Transfer 2012;113:850–8.
[23] Grechko M, Aseev O, Rizzo TR, Zobov NF, Lodi L, Tennyson J, et al. Stark coefficients for highly excited rovibrational states of $H_2O$. J Chem Phys 2012;136:244308.
[24] Petrignani A, Berg M, Wolf A, Mizus II, Polyansky OL, Tennyson J, et al. Visible intensities of the triatomic hydrogen ion from experiment and theory. J Chem Phys 2014;141:241104.
[25] Zak EJ, Tennyson J, Polyansky OL, Lodi L, Zobov NF, Tashkun SA, et al. Room temperature line lists for $CO_2$ symmetric isotopologues with ab initio computed intensities. J Quant Spectrosc Radiat Transf 2017;189:267–80.
[26] Zak EJ, Tennyson J, Polyansky OL, Lodi L, Zobov NF, Tashkun SA, et al. Room temperature line lists for $CO_2$ asymmetric isotopologues with ab initio computed intensities. J Quant Spectrosc Radiat Transfer 2017;203:265–81.
[27] Rinsland CP, Benner DC. Absolute intensities of spectral lines in carbon dioxide bands near 2050 cm$^{-1}$. Appl Opt 1984;23:4523–8.
[28] Gordon IE, Rothman LS, Hill C, Kochanov RV, Tan Y, Bernath PF, et al. The HITRAN2016 molecular spectroscopic database. J Quant Spectrosc Radiat Transfer 2017;203:3–69.
[29] Benner DC, Devi VM, Sung K, Brown LR, Miller CE, Payne VH, et al. Line parameters including temperature dependence of air- and self-broadened line shapes of $^{12}C^{16}O_2$: 2.06-$\mu$m region. J Mol Spectrosc 2016;326:21–47.
[30] Toth RA, Brown LR, Miller CE, Devi VM, Benner DC. Line strengths of $^{12}C^{16}O_2$: 4550 – 7000 cm$^{-1}$. J Mol Spectrosc 2006;239:221–42.
[31] Wang J, Sun YR, Tao LG, Liu AW, Hua TP, Meng F, Hu SM. Comb-locked cavity ring-down saturation spectroscopy. Rev Sci Instrum 2017;88:043108.
[32] Wang J, Sun YR, Tao LG, Liu AW, Hu SM. Communication: Molecular near-infrared transitions determined with sub-kHz accuracy. J Chem Phys 2017;147:091103.
[33] Lu Y, Liu AW, Li XF, Wang J, Cheng CF, Sun YR, Lambo R, Hu SM. Line parameters of the 782 nm band of $CO_2$. Astrophys J 2013;775:71.
[34] Zhao XQ, Wang J, Liu AW, Zhou ZY, Hu SM. High precision cavity ring down spectroscopy of 6v3 overtone band of $^{14}N_2{}^{16}O$ near 775 nm. Chin J Chem Phys 2017;30:487–92.
[35] Cygan Agata, Wcisło Piotr, Wojtewicz Szymon, Masłowski Piotr, Hodges JosephT, et al. One-dimensional frequency-based spectroscopy. Opt Express 2015;23:14472–86.
[36] Ngo NH, Lisak D, Tran H, Hartman JM. An isolated line-shape model to go beyond the Voigt profile in spectroscopic database and radiative transfer codes. J Quant Spectrosc Radiat Transfer 2013;129:89–100.
[37] Casa G, Wehr R, Castrillo A, Fasci E, Gianfrani L. The line shape problem in the near-infrared spectrum of self-colliding $CO_2$ molecules: Experimental investigation and test of semiclassical models. J Chem Phys 2009;130:184306.
[38] Long DA, Bielska K, Lisak D, Havey DK, Okumura M, Miller CE, Hodges JT. The air-broadened, near-infrared $CO_2$ line shape in the spectrally isolated regime: Evidence of simultaneous Dicke narrowing and speed dependence. J Chem Phys 2011;135:064308.
[39] Rautian SG, Sobel'man II. The effect of collisions on the Doppler broadening of spectral lines. Sov Phys Usp 1967;9:701–16.
[40] Lance B, Blanquet G, Walrand J, Bouanich JP. On the speed-dependent hard collision lineshape models: application to $C_2H_2$ perturbed by Xe. J Mol Spectrosc 1997;185:262–71.
[41] Gamache RR, Roller C, Lopes E, Gordon IE, Rothman LS, Polyansky OL, et al. Total internalpartition sums for 166 isotopologues of 51 molecules important in planetary atmospheres: application to HITRAN2016 and beyond. J Quant Spectrosc Radiat Transfer 2017;203:70–87.
[42] Toth RA, Brown LR, Miller CE, Devi VM, Benner DC. Spectroscopic database of $CO_2$ line parameters: 4300-7000 cm$^{-1}$. J Quant Spectrosc Radiat Transfer 2008;109:906–21.
[43] Karlovets EV, Campargue A, Mondelin D, Béguier S, Kassi S, Tashkun SA, Perevalov VI. High sensitivity cavity ring down spectroscopy of $^{18}O$ enriched carbon dioxide between 5850 and 7000 cm$^{-1}$: I. Analysis and theoretical modeling of the $^{16}O^{12}C^{18}O$ spectrum. J Quant Spectrosc Radiat Transfer 2013;130:116–33.
[44] Hirschfelder JO, Curtiss CF, Bird RB. Molecular theory of gases and liquid. New York: Wiley; 1966.
[45] Boudjaadar D, Mandin JY, Dana V, Picqué N, Guelanchvili G, Régalia-Jarlot L, et al. $^{12}C^{16}O_2$ line intensity FTS measurements with 1% assumed accuracy in the 1.5-1.6 $\mu$m spectral range. J Mol Spectrosc 2006;238:108–17.